

# NUMERICAL ANALYSIS OF CONTROLLING SEPARATION IN AXIAL CASCADES BY EXCITATION OF PERIODICAL INCOMING WAKE

FEI LIU, JIABING WANG AND KEQI WU

*School of Energy and Power Engineering,  
Huazhong University of Science and Technology,  
Wuhan, Hubei, 430074, P. R. China  
hustliufei@tom.com*

(Received 24 August 2007)

**Abstract:** Numerical analysis has been performed of time-space structures in a large turning angle axial cascade subject to unsteady incoming wake excitation. The results have shown that intentional unsteady excitation could increase the cascade's time-averaged performance. As a result, the vortex structures corresponding to the external exciting frequency are strengthened and other disordered vortices are involved, so that the separation structures of the suction surface are translated from disorder to order. Two interaction regimes between incoming periodic wakes and separation structures are analyzed, indicating that turbulent kinetic energy can enhance momentum interchange and that wave-vortex resonance can promote rolled-up and plus-minus pairing of vortices. Based on these, responses of separation structures from two periodic incoming wake regimes are compared. The feasibility of far-field noise reduction in ducting fans by using periodic incoming wake is considered.

**Keywords:** unsteady excitation, compressor cascade, separation control, incoming wake, vortex shedding

## *Nomenclature*

$c$  – chord length  
 $u$  – velocity  
 $P$  – total pressure  
 $p$  – static pressure  
 $T$  – periodic time  
 $x$  – axial direction  
 $y$  – pitch direction  
 $\beta$  – flow angle  
 $f$  – frequency  
 $\xi$  – pressure drop coefficient  
PS – pressure surface  
SS – suction surface

## 1. Introduction

Active flow separation control is of great concern in numerous engineering applications. The phenomena of flow separation and re-attachment are accompanied by large energy losses, influencing the performance of fluid machinery and imposing severe limitations on the operation and design of many fluid flow devices [1]. Strong, adverse pressure gradient (or local surface curvature [2]) and decreased momentum inside a boundary layer are well-known critical factors underlying boundary layer separation. Unfortunately, adverse pressure gradient is generally stronger in axial flow compressors than in other fluid machines. Axial flow compressors mainly rely on aerodynamic diffusion to increase pressure. Since the adverse pressure gradient associated with diffusion becomes especially strong at high loading levels of modern designs, unsteady separation is inevitable. This has a negative impact on the stall margin, efficiency and pressure-increasing capability.

Early works on separation control were focused on passive control, choosing optimal airfoil and nozzle geometries to delay separation. In recent years, with the development of the flow visualization technology, it has been realized that complex vortex structures appear during the transition from shear flow to turbulence, which have significant effects on many aspects of flow performance, including the change of noise radiation, lift and drag. In addition, the evolution of vortex structures is sensitive to the external special frequency, which has induced the idea of controlling vortex structures with weak unsteady excitation [3]. Most recently, wave adjustment and vortex control have become new ways to transform flow vortex structures from stochastic unsteady to comparatively periodic, changing their impact from a disadvantage to an advantage.

Numerous experiments and CFD studies carried out in order to control stall flow of airfoil with unsteady excitation in the external flow field, have shown that the external unsteady effect is capable of enhancing lift and reducing drag. However, the flow environments of airfoil and a compressor are different. Airfoil is a single-object system and unsteady forcing must be artificially excited, while a compressor is a multi-object system. To the authors' knowledge, little research has been performed on separation control through unsteady excitation in axial flow compressors [4]. The present paper aims at finding a new way to achieve separation control in axial flow compressors. Generally speaking, the relative wake movement from upstream blade rows of an axial compressor may be deemed an "unsteady actuator" of the unsteady separated flow field of the adjacent downstream blades. In the present paper, periodic inflow wake is used to simulate the above-mentioned unsteady excitation to research the mechanism of controlling separated flow by external unsteady effects.

Unsteady wake, characterized by a defect in the mean velocity profile and locally intensified turbulence intensity, dramatically influences the unsteady behavior of turbulent separation bubbles. The dynamics of unsteady flow's behavior are usually related to unwanted phenomena such as energy loss, structural vibration and sound radiation. Accordingly, in-depth analysis of the underlying complex interactions between turbulent separation bubbles and unsteady wake is sorely needed [5]. Schobeiri *et al.* [6] studied experimentally the effects of periodic unsteady wake flow

on the boundary layer's development, separation and reattachment. The unsteady periodic flow caused by the relative motion of rotor and stator rows and its influence on the compressor cascade were simulated by a moving bar-type wake generator with a bar diameter of 2 mm. The wake impingement introduces fluctuation kinetic energy from its vortex core into the boundary layer, in an attempt to energize it and reverse the tendency to separate. Zheng and Zhou [4, 7] investigated the so-called "wake impact effect", a new to control unsteady separated flow in compressors. Their results showed that a disordered unsteady separated flow could be effectively controlled with an external periodic effect in a wide range of incidences, resulting in enhanced time-averaged aerodynamic performance of an axial compressor cascade. The effects of unsteady excitation's frequency, amplitude and location were investigated in detail. Hilgenfeld and Pfitzner [8] investigated the effects of passing wake on boundary layer development near the suction side of a highly loaded linear compressor cascade. The incoming wakes clearly influenced the unsteady boundary layer's development. The time-mean momentum thickness values were reduced compared with the steady ones and the potential for loss reduction due to wake passing effects was thus made clear.

The objective of the present paper is twofold. One is to investigate the performance and flow structures resulting from various inlet velocity profiles and fluctuation frequencies and identify the improvement in flow separation excited by external periodicity. The mechanism of interaction between incoming excitation and the flow structure is analyzed on the basis of the computational results. The other objective is to compare the unsteady characteristics with and without intentional external excitation in order to identify the relation between the external frequency and the characteristic frequency of the internal flow for preferable excitation. With these objectives in view, a numerical simulation of unsteady internal flow characteristics is presented in a single-stage axial compressor cascade. We have used the periodicity of incoming wake as unsteady excitation to weaken the separation inside the cascade. Considering the complexity of flows in axial compressors, we have only considered a two-dimensional (2D) case.

## 2. Numerical methods

### 2.1. Turbulence model

Considering the expensive computational resources required for direct numerical simulation (DNS), large eddy (LES) and unsteady Reynolds-averaged Navier-Stokes (URANS) simulations are interesting alternative approaches. In LES, all dynamics of turbulent eddies above a cutoff filter (twice the mesh size) are resolved, while only small-scale fluctuations are modeled. In URANS, all turbulent fluctuations are modeled, but large-scale rotational motion is resolved as an unsteady phenomenon. Thus, URANS is aimed at capturing the first few fundamental frequencies only and models random motions using a standard turbulence closure [9]. In flows dominated by discrete-frequency large-scale structures that URANS can resolve, it is conceivable that URANS may provide solutions of reasonable accuracy with moderate computational effort. As discussed earlier, LES is known for its higher temporal and spatial accuracy. For the problems in which the discrete frequency does not dominate the flow structures, LES could give improved accuracy with reasonable computational resources.

Sometimes, computational results cannot confirm with the anticipation by solving URANS. For instance, while controlling the flow separation in a backward-facing step, an external periodic perturbation is generally introduced to weaken the separation structure. Saric *et al.* [1] studied the turbulent flow over a backward-facing step perturbed periodically by alternating blowing/suction through a thin slit using LES, DES and URANS techniques. Comparing the computational results with the experimental data, the closest agreement with experiment was obtained with LES and DES, whereas the URANS computations showed a weaker sensitivity to the external perturbation.

The present research is focused on the response of multi-scale vortex structures to external periodic perturbation, with the LES technique chosen for unsteady computations. The filtering N-S equations, which can describe coherent vortex movement in flow structures, are solved by the Finite Volume Method (FVM). Additionally, the interaction between large and small vortexes is modeled. Resolving large eddies only enables using a much coarser mesh and greater time steps than in DNS. Nevertheless, LES requires substantially finer meshes than those typically used for RANS calculations. LES must be run for a sufficiently long flow time in order to obtain stable statistics of the modeled flow.

Upon filtering, the two-dimensional incompressible unsteady Navier-Stokes equations read as follows:

$$\frac{\partial \bar{u}_i}{\partial x_i} = 0, \tag{1}$$

$$\frac{\partial \bar{u}_i}{\partial t} + \frac{\partial(\bar{u}_i \bar{u}_j)}{\partial x_j} = -\frac{1}{\rho} \frac{\partial \bar{p}}{\partial x_i} + \frac{\partial}{\partial x_j} \left( \mu \frac{\partial \sigma_{ij}}{\partial x_j} - \tau_{ij} \right), \tag{2}$$

where  $\sigma_{ij}$  is the stress tensor due to molecular viscosity and  $\tau_{ij}$  is the subgrid-scale stress defined approximately by employing Boussinesq's formulation based on the SGS turbulent viscosity, modeled using the Smagorinsky formulation [1].

Steady computational results using the standard  $k-\varepsilon$  two-equations turbulent model are treated as the initial value of the unsteady LES solution. The well-known SIMPLE algorithm is applied for coupling the velocity and pressure fields. Convective transport of all variables is discretized with a second-order central difference scheme. Time discretization is accomplished by applying the second order method. The time step of the unsteady solution is  $5 \cdot 10^{-5}$  s.

## 2.2. Computational conditions and grid generation

The large turning angle axial cascade for our study of external frequency excitation has been taken from reference [10]. It is of the NACA 65 series, with geometric parameters given in Table 1.

**Table 1.** Geometric parameters of the cascade

chord $b$ [mm]	100	aspect ratio $h/b$	1.0	inlet metal angle [deg]	48.19
solidity $b/t$	1.364	stagger angle [deg]	18.18	outlet metal angle [deg]	-11.81

Periodic unsteady incoming wake has sometimes been simulated with the translational motion of a wake generator with a series of cylindrical rods. Schobeiri [6] obtained approximately sinusoidal incoming velocity distribution by translating thin

cylindrical rods of different spacing intervals with the uniform inlet velocity. His results demonstrated the closer an inlet velocity distribution is to a sinusoid, the better the control effect of separation. Hilgenfeld [8] also studied the effect of periodical wake from upstream rows on the flow characteristic of a compressor cascade, using moving cylindrical rods as a wake generator and comparing the effects of various spacing intervals.

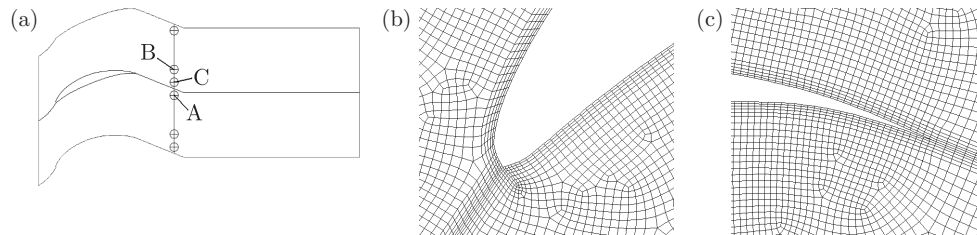


**Figure 1.** Model and grid schemata: (a) the model structure, (b) near the leading edge, (c) near the trailing edge

In order to make the best use of the available computer resources, we have used the processing mode of a single flow passage in an axial compressor by specifying a periodical hypothesis and using a periodical boundary condition. Initial grid sensitivity tests have shown the grid size to influence the solution. Since separated flows are usually characterized by free shear layers as well as strong viscous effects, it was deemed necessary to achieve a highly refined mesh for regions adjacent to blade surfaces [11]. A hexahedral structural grid was introduced throughout the computing domains, helpful in solution and analysis. The total cell number was about two hundred thousand, which is not much and allows for further mesh refinement by adaptation based on definite solution. The model and the grid are schematically shown in Figure 1.

While implementing the unsteady excitation, the wake generator was simplified in order to emphasize the mechanism of unsteady external excitation. The sinusoidal distribution of inlet velocity fluctuation with time was introduced instead of the function of motor cylindrical rods. The traveling wavelength of inlet velocity was additionally assumed to equal cascade spacing, *i.e.* the number of wake generators was assumed to equal the number of cascades. The boundary types contributing to the solution were inlet velocity and outlet static pressure. In order to ensure matching between the inlet velocity condition and the assumed distribution, user-defined functions (UDF) were accepted while allocating inlet velocity to specify inlet velocity profiles corresponding to the assumed incoming wake conditions.

### 3. Discussion of results

The research results have shown that there are vortices of various scales in the time-space structures of the unsteady separation region, including shedding vortices, which are dominant and significantly react to correlative unsteady characteristics of the separated flow [3]. We will therefore focus on the characteristic frequency of vortex shedding and treat it as the reference frequency of unsteady excitation. The relative exciting frequency is defined with the  $\bar{f}_f = f_f / f_{shed}$  formula, where  $f_f$  is the

external forcing frequency and  $f_{\text{shed}}$  is the characteristic frequency downstream of cascade. Two directional motions of the wake generator are carried out, where “to PS” represents the wake’s motion from SS to PS, while the direction of “to SS” is reverse. The computational results have shown that the frequency of vortex shedding from cascade PS is 122 Hz at the assumed attack angle. The unsteady flow characteristic without external excitation will be analyzed in detail.

### 3.1. Performance effects of external excitation

Having obtained the time-domain distribution of total pressure at the cascade’s outlet section, the pressure loss is judged by comparing the inlet and outlet time-averaged total pressure. The pressure drop coefficient is defined as  $\xi = (\bar{P}_{\text{out}} - \bar{P}_0) / \bar{p}_{v0}$ , where  $\bar{P}_{\text{out}}$  represents the time-averaged total pressure at the cascade’s outlet section,  $\bar{P}_0$  and  $\bar{p}_{v0}$  respectively standing for the inlet time-averaged total pressure and dynamic pressure.

As shown in Table 2, different exciting parameters result in differences in time-averaged performance of the cascade. It appears that intentional external excitation increases the flow deflection to some extent; the flow direction at the outlet of the cascade is closer to the axial direction. The total pressure loss decreases with excitation, about 20% at the amplitude peak. These improvements demonstrate that the effective unsteady excitation enhances the time-averaged performance in a cascade.

**Table 2.** Comparison of time-averaged performance in a cascade

direction	$\bar{f}_f$	$\Delta\beta$	$\xi$	loss reduction
without excitation		56.66	0.098	
to PS	1	67.2	0.082	16.3%
to SS	1	62.12	0.08	18.4%
to PS	2	66.95	0.078	20.4%
to PS	0.5	59.97	0.083	15.3%

### 3.2. Mechanism between incoming periodical wakes and flow structures

A vorticity contour of vortex shedding from a pressure surface is shown in periodic time in Figure 2. From the view of the time interval, the vortex shedding structure of the trailing edge is clearly periodical, because of the fluent and smooth flow characteristic near PS. In terms of vortex structures, the vortex near SS and the trailing edge is partly involved in the course of PS vortex shedding, but the involved quantity is hardly periodic. Near SS, a large camber and an attack angle bring about a very complex large-scale separation flow, suggesting that there is no single dominant characteristic frequency. The same frequency characteristics (*i.e.* no periodic vortex shedding from SS) is also suggested by the total pressure spectrum of Figure 11a. In the light of the zero vorticity theorem [3], the separation point is located at 40% of the axial chord along the suction surface. Later, the fluid before the separation point re-attaches the suction surface as it travels and so the separation bubble is formed. The negative vorticity region, by which the positive vorticity fluid is involved, is large near

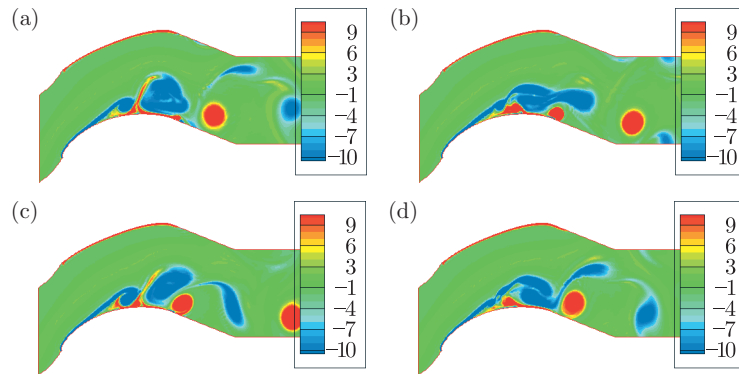


**Figure 2.** Vorticity contour at various times without external excitation:  
 (a)  $t = 0$ , (b)  $t = 1/4T$ , (c)  $t = 1/2T$ , (d)  $t = 3/4T$

the re-attachment point. When the aggregation of vorticity is almost saturated, the aggregated vortex structures are shed towards the downstream side. Therefore, the SS vortex shedding structures, which merge with PS shedding vortices and separation bubble vortices, respectively, are more complicated than the PS ones.

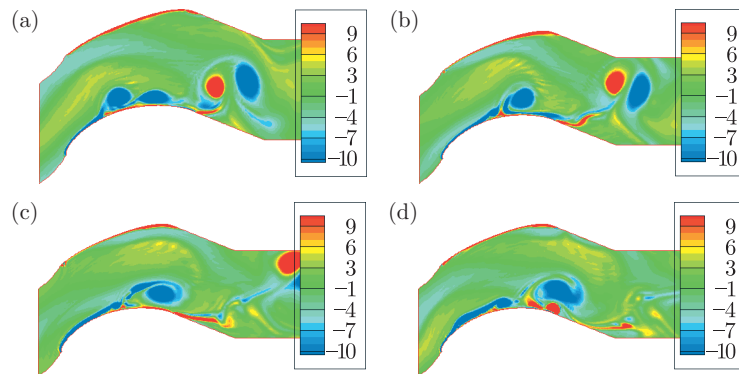


**Figure 3.** Instantaneous vorticity contours (to PS,  $\bar{f}_f = 1$ ):  
 (a)  $t = 0$ , (b)  $t = 1/4T$ , (c)  $t = 1/2T$ , (d)  $t = 3/4T$

Instantaneous vorticity distributions of two regimes, a “wrapping” regime and a “cutting” regime, produced by different incoming wakes [12] are shown in Figures 3 and 4. The distribution of Figure 3 (the “wrapping” regime) corresponds to the conditions in which the wake headstream propagates from SS to PS, while the direction in Figure 4 is opposite. In the “wrapping” regime of Figure 3, the unsteady wake-cascade interaction is characterized by the outward motion of the separation bubble of the suction surface prior to impact with the wake and the subsequent wrapping of the unsteady wake around the bubble. In the “cutting” regime, the separation bubble is disturbed by the incoming unsteady wake at the separation edge with the inward motion of the separation bubble onto the suction surface. Using the aforementioned zero vorticity theorem, the separation bubbles of the two regimes are periodically weakened or partly controlled. The separation position of that of the “cutting” regime is closer to the trailing edge, as the separation bubble is wiped off by the incoming

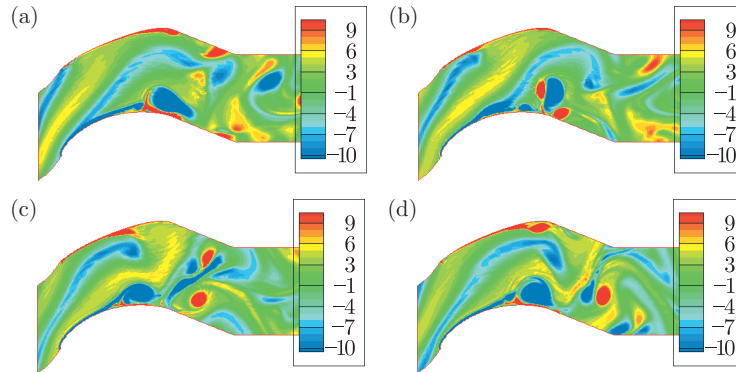


**Figure 4.** Instantaneous vorticity contours (to SS,  $\bar{f}_f = 1$ ):  
 (a)  $t = 0$ , (b)  $t = 1/4T$ , (c)  $t = 1/2T$ , (d)  $t = 3/4T$

wake. The obtained calculation results are in accordance with the solution obtained by Chun [12].

Moreover, considering the responses of separation near SS and the trailing vortex shedding structures to the incoming wake's periodicity shown in Figure 4, the separation bubble interacts more compactly with the incoming wake in the "cutting" regime, but the incoming periodicity is shadowed further, which results in the vortex and separation structures having less sensibility to wake periodicity. This is why the flow structure shown in Figure 4 is more irregular than that of Figure 3. Under conditions corresponding to Figure 3, the separation region is apparently more sensitive to incoming periodicity owing to the motion regime of the wake strip, which just ensures that the plus-minus vorticity structures in the separation and trailing vortex region evolve into vortex pairs as the intentional external exciting frequency interacts with the dominant modality of these regions. As a result, the vorticity distribution is more quasi-ordered than the original flow structure without external excitation. When the external frequency is doubled, as shown in Figure 5, the wake strip in a single flow passage becomes shorter, which may render the vortex structures of the separation and trailing region more sensitive to the incoming wake periodicity. As a result, the plus-minus vorticity structures originating from SS and PS will match pairs more easily and follow each other more tightly, so that apparent periodicity tends to emerge. All of these factors will conduce to reduction of the re-attachment length and the size of the separation bubble [12]. Tong [3] has suggested that the rolled-up and plus-minus pairing of vortices of the separation shear layer contribute to effects facilitating small-scale flow transitions, an ideas which can be used to control flow separation.

As shown in Figure 6, the time-averaged velocity distribution near the separation point ( $x/c_x = 40\%$ ) is slightly affected by the incoming wake. But downstream of the separation point, the magnitude of time-averaged velocity near SS is increased remarkably by the effect of incoming turbulent intensity, while the range of low-energy fluid shrinks toward the cascade's surface and the thickness of the boundary layer decreases. The effect of unsteady wake on the RMS value of streamwise velocity fluctuations is shown in Figure 7, where fluctuation distributions at two streamwise positions along the pitch direction are given. The level of fluctuating velocity is signif-

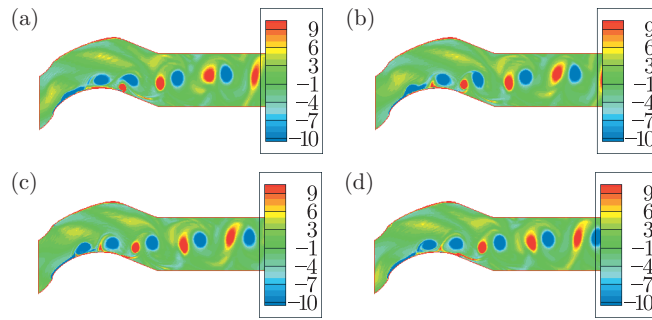


**Figure 5.** Instantaneous vorticity contours (to PS,  $\bar{f}_f = 2$ ):  
(a)  $t = 0$ , (b)  $t = 1/4T$ , (c)  $t = 1/2T$ , (d)  $t = 3/4T$

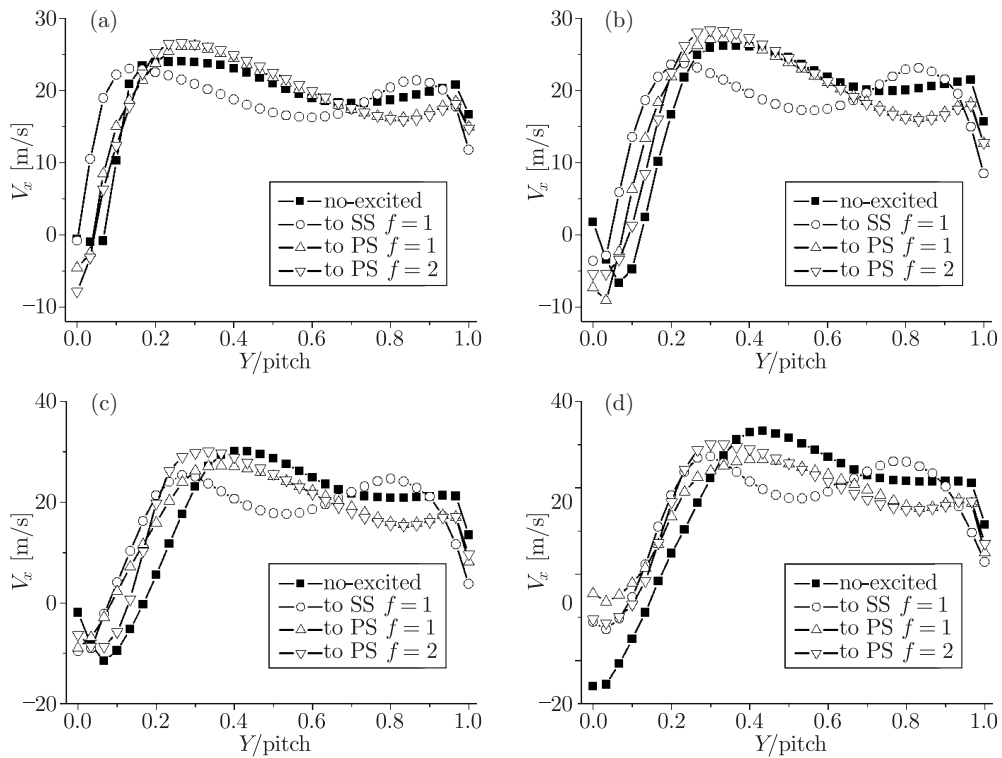


**Figure 6.** Time-averaged streamwise velocity along the pitch direction:  
(a)  $x/c_x = 40\%$ , (b)  $x/c_x = 55\%$ , (c)  $x/c_x = 70\%$ , (d)  $x/c_x = 85\%$

icantly affected by the unsteady wake after the separation point, where the rolled-up vortices have just formed. An inspection of profiles within the separation bubble discloses that the velocity distributions disturbed by the unsteady wake have higher fluctuation levels than those without the unsteady wake. Comparing the incoming wake regimes, the regime corresponding to “to SS” induces more severe velocity fluctuations than that the “to PS” regime, which confirms the results of Chun [12]. The contours of Reynolds stress,  $\overline{u'v'}/U_0^2$ , around the cascade with and without incoming wake excitation are shown in Figure 8. The contour of Reynolds stress without excitation shows its considerable magnitude in the cascade’s rear and in the wake, which

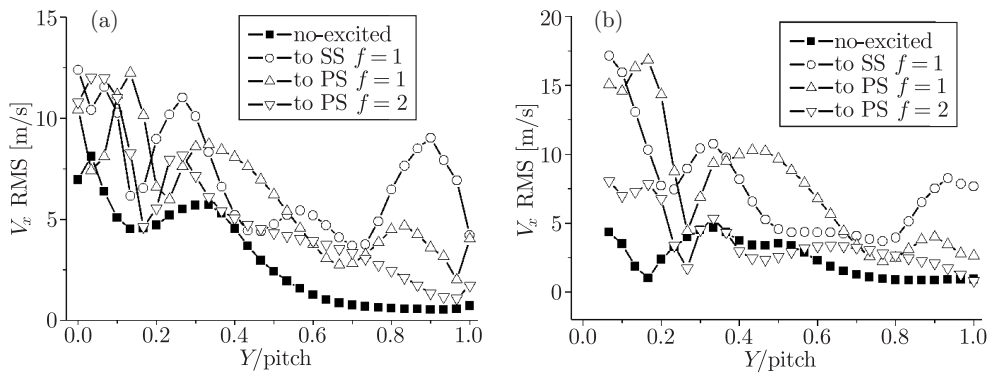


Figure 7. Streamwise velocity fluctuaton  $V_x$  RMS: (a)  $x/c_x = 70\%$ , (b)  $x/c_x = 85\%$

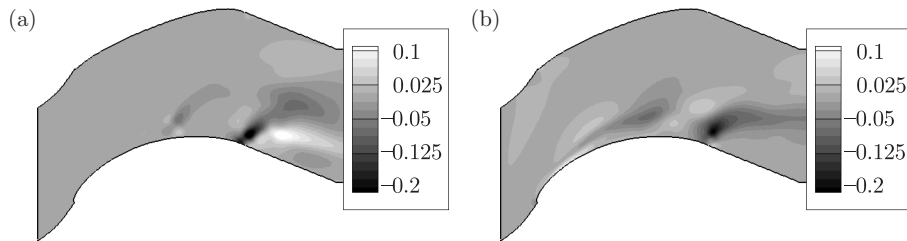


Figure 8. Contour of  $\overline{u'v'}/U_0^2$ : (a) origin, (b)  $\bar{f}_f = 2$

indicates periodic vortex shedding from the cascade's pressure surface. It is clearly visible in Figure 8b that the high peak of Reynolds stress on the pressure surface near the cascade's trailing edge has been removed and the magnitude of Reynolds stress in the wake of the airfoil is reduced in comparison with the results without external excitation. The plus-minus vortices shed from the trailing edge follow each other more tightly, an effect of given external frequency. Therefore, the width and intensity of the cascade's wake are reduced. Additionally, the turbulent intensity of incoming wake results in an increment of Reynolds stress near the separation region. As a result, the velocity fluctuation becomes more severe, the momentum interchange is strengthened and the large scale of the inverse flow and separation structures can be periodically restrained.

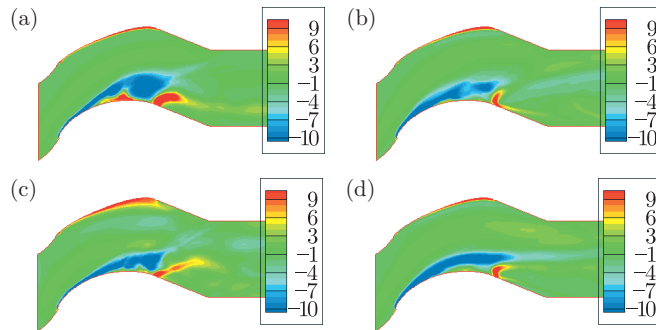
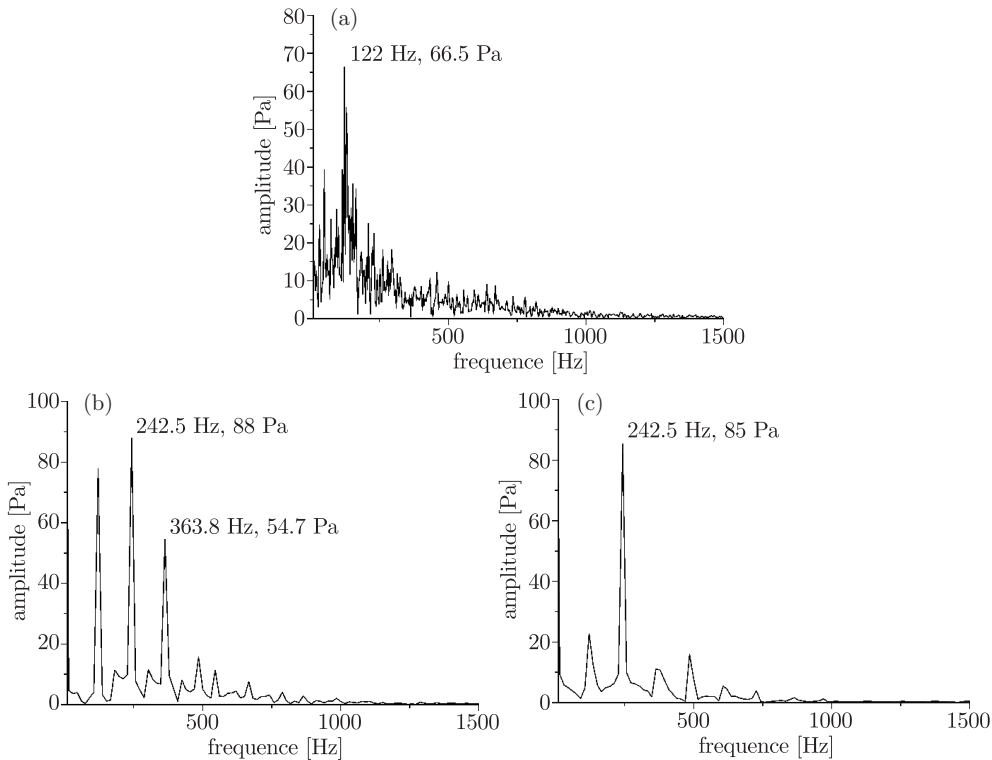


Figure 9. Time-averaged vorticity contours with and without external excitation: (a) origin, (b) to PS,  $\bar{f}_f = 1$ , (c) to SS,  $\bar{f}_f = 1$ , (d) to PS,  $\bar{f}_f = 2$

Time-averaged vorticity contours with and without external excitation are shown in Figure 9. The effective external excitation removes the plus-minus vorticity peak towards the suction surface, so that the size of the separation bubble is reduced sharply. Especially under the conditions of external excitation corresponding to Figure 9d, the more reasonable external frequency produces more compact vortex-shedding structures.

**3.3. Unsteady characteristics with and without external excitation**



**Figure 10.** Total pressure spectrum at point A

The total pressure spectra at two observation points are shown in Figures 10 and 11 under different incoming wake effects. As shown in Figure 11a, no external excitation and large scale of separation produce a broad band characteristic of the total pressure spectrum at point B, located just downstream of the separation bubble. It is the same as per Figure 2, in which vortex shedding from the trailing edge is non-periodical. At points other than B, including point A, there is a prominent discrete signal and a broad-band signal with an amplitude corresponding to the smaller vortices around it in the total pressure spectrum. After effective external frequencies have been introduced, the beneficial influence of excitation is clearly visible. The flow structure downstream of the separation region becomes more quasi-ordered. Therefore, the amplitudes of the discrete frequency corresponding to coherent vortex structures are enhanced and those of the broad-band frequency corresponding to the lesser vortex structures are weakened. These results suggest that the vortex

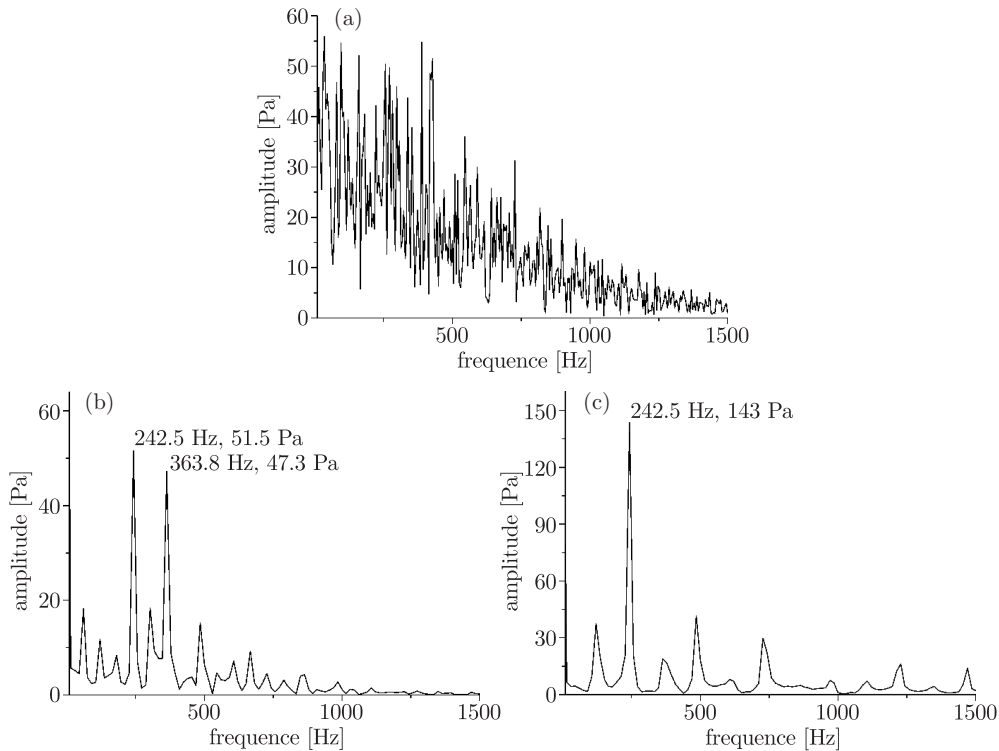


Figure 11. Total pressure spectrum at point *B*

shedding structures corresponding to the external exciting frequency are strengthened and other vortices are entrained or partly merged.

The spectrum of Figure 11c shows that more disordered vortices are involved in the interaction between external excitation and the fluid's dominant instability frequency than that of Figure 11b. In other words, the interaction between the incoming traveling wave and the vortex structure becomes stronger and the vortex matched pairs are more manifest. The velocity fluctuation with the excitation becomes clearly periodical in the velocity phasic chart shown in Figure 12. Because point *C* is located at the rear side of the trailing edge, the matched pairs of vortices shed in Figure 12c are more compact than those of Figure 12b and the wake's width is confined to a narrow range, so that the velocity fluctuation is less distinct at this point (in both directions).

The computational results reveal that, under certain conditions, unsteady external excitation can improve the vortex structures within the region of SS flow separation and cascade wake. The vortices corresponding to the external effective frequency are enhanced. As a result, other vortices are entrained by the strengthened vortices, leading to combination of the disordered vortices [7].

#### 4. Conclusions

Intentional external excitation increases the flow deflection to some extent, and the flow direction at the outlet of the cascade is closer to the axial direction. Under

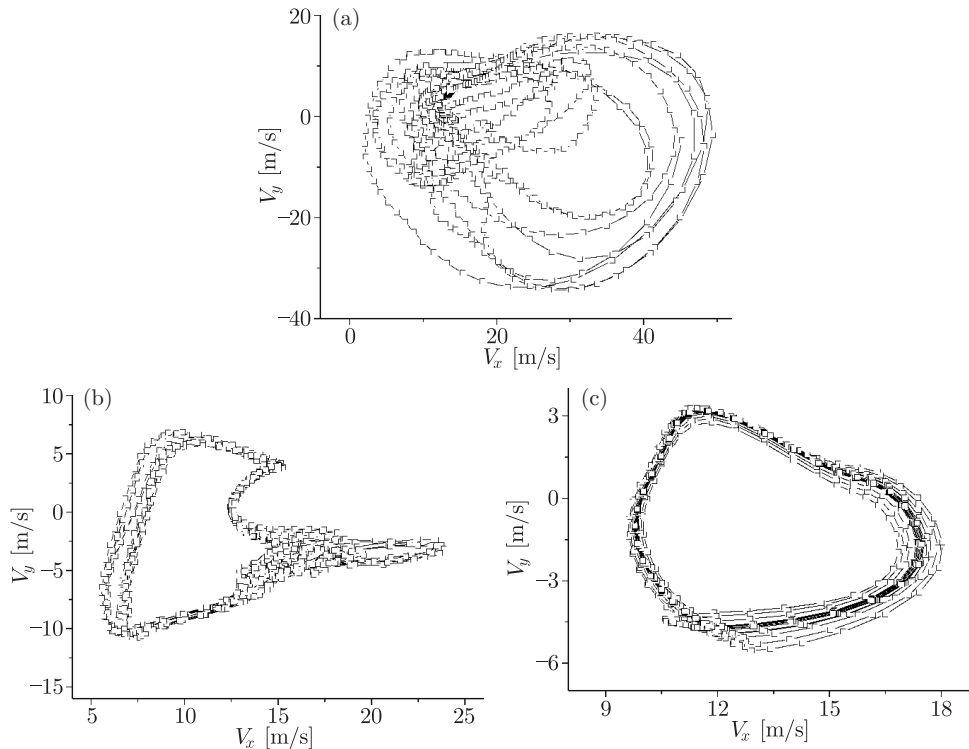


**Figure 12.** Velocity phasic chart at point C: (a) without excitation, (b) to PS  $\bar{f}_f = 1$ , (c) to PS  $\bar{f}_f = 2$

such excitation, the total pressure loss is reduced by about 20% at the amplitude peak. Effective unsteady excitation improves the time-averaged performance of cascades.

Shedding vortex structures from the trailing edge is clearly periodical. Near SS, a large camber and an attack angle bring about a very complicated large-scale separation flow, suggesting that there is no single dominant characteristic frequency. Therefore, the SS vortex-shedding structures, which merge with PS shedding vortices and separation bubble vortices, respectively, are more complex than those of PS. The confinement functions of the separation structure from the incoming periodical wake is twofold. On the one hand, the turbulent intensity of incoming wake increases the Reynolds stress near the separation region. The velocity fluctuation thus becomes more severe and the momentum interchange is strengthened. The large scale of the inverse flow and separation structures can be prevented intermittently. On the other hand, the wave-vortex resonance interaction between periodical traveling waves and the separated vortex structures may promote rolled-up and plus-minus pairing of vortices. The matched-pair structures of shedding vortices are thus more compact and the wake's width is confined. Based on these mechanisms, two interaction regimes of vortex structures and incoming wakes are discernible, a "cutting" regime and a "wrapping" regime. The separation structures of the latter are more sensitive to incoming periodicity.

The vortices corresponding to the external effective frequency are enhanced. As a result, other vortices are generated by the strengthened vortices, leading to

combination of the disordered vortices. By intentionally introducing periodical wake excitation, flow structures can be translated from disorder to order and flow separation can be effectively controlled, with flow enhancement in view.

## 5. Further considerations

In axial turbomachinery, the flow characteristic of the boundary layer is effectively improved by intentional external excitation. At the same time, the time-averaged performance is increased and the flow structures become more quasi-ordered by merging other vortices. It also follows from the above-mentioned total pressure spectrum that the quasi-ordered flow excited by external frequency makes the fluctuation of parameters discrete. The parameters include discretization of the fluid force imposed on blade surfaces, which may induce apparent blade vibration.

With respect to the far-field noise, due to the noise radiated from a low-speed axial fan being chiefly broad-band noise induced by vortices of various scales, enhancing the flow's dominant frequency and merging other vortices by flow control with unsteady external excitation will reduce broad-band noise in a wide frequency range. However, it is inevitable that the magnitude of tonal noise corresponding to external frequency will be increased. In an axial fan with a middle- or low-pressure head, especially in a single-rotor ducting fan, the far-field fan noise is reducible to a low level owing to the attenuation function of tonal noise by acoustic impedance passing through the duct [13]. Therefore, it is feasible that the total noise level will be reduced by using unsteady excitation of the incoming wake to merge the broad-band component of the noise. Further research based on this idea will be carried out in the future.

### Acknowledgements

This work was supported by grants from the National Natural Science Foundation of China (No. 51076035) and from the Ph.D. Programs Foundation of the Ministry of Education of China (No. 20100487036).

### References

- [1] Saric S, Jakirlic S and Tropea C 2005 *ASME J. Fluids Engng* **127** (5) 879
- [2] Pack L G and Seifert A 2000 *Dynamics of Active Separation Control at High Reynolds Numbers, AIAA Paper* **2000-0409**
- [3] Tong B G, Zhang B X and Cui E J 1993 *Unsteady Flow and Vortex Motion*, Beijing (in Chinese)
- [4] Zheng X Q, Zhou X B and Zhou S 2005 *ASME J. Turbomachinery* **127** (3) 489
- [5] Chun S, Liu Y Z and Sung H J 2007 *J. Fluids and Structures* **23** 85
- [6] Schobeiri M T and Oztiirk B 2007 *ASME J. Turbomachinery* **129** (1) 92
- [7] Zheng X Q, Hou A P and Zhou S 2003 *Acta Mechanica Sinica* **35** (5) 599 (in Chinese)
- [8] Hilgenfeld L and Pfitzner M 2004 *ASME J. Turbomachinery* **126** (4) 493
- [9] Saha A K and Acharya S 2005 *ASME J. Turbomachinery* **127** (2) 310
- [10] Song Y P, Chen F, Yang J and Wang Z 2006 *ASME J. Turbomachinery* **128** (2) 357
- [11] Bbadebo S A, Cumpsty N A and Hynes T P 2005 *ASME J. Turbomachinery* **127** (2) 331
- [12] Chun S and Sung H J 2002 *Experiments in Fluids* **32** 269
- [13] Wang Q H, Wang N, Yu D Z and Tang Y H 1999 *Chinese J. Engng Thermophysics* **20** (1) 41 (in Chinese)